Korean J. of Chem. Eng., **14**(1), 41-48 (1997)

LONG-WAVE INSTABILITIES OF FILM FLOW UNDER AN ELECTROSTATIC FIELD
: TWO-DIMENSIONAL DISTURBANCE THEORY

Hyo Kim

Department of Chemical Engineering, Seoul City University,
90 Jeonnong-Dong, Dongdaemun-Gu, Seoul 130-743, Korea
(Received 18 July 1996 • accepted 16 December 1996)

Abstract – The free-surface behavior of a viscous liquid layer flowing down an inclined plane by gravity and interacting with an overlying uniform electrostatic field is examined in the limit of long-wave approximation. Both linear and nonlinear stability analyses are performed to address two-dimensional surface-wave evolution initiating from a flat interface. The growth of a periodic disturbance is first investigated for a linear analysis, and then to examine the nonlinear surface-wave instabilities the evolution equation for film height is solved numerically by a Fourier-spectral method. For small evolution time the calculated nonlinear modes of instability are consistent with the results obtained from the linear theory. The effect of an electrostatic field increases the wavenumbers showing a maximum linear growth rate as well as a cutoff. A significant phenomenon as Reynolds number is increasing is the appearance of the catastrophic surface waves in the long run whenever any initial wavenumber making a traveling wave linearly unstable is employed into the initial simple-harmonic disturbance.

Key words: *Film Flow, Electrostatic Field, Instability, Fourier-Spectral Method, Growth Rate*

INTRODUCTION

The behavior of the thin liquid-film flow has attracted much attention for many years because the thin layer of liquid acts an important role in many engineering processes due to its high transfer surface of heat and mass in comparison with the volume of through-flow. If the flowing layer is electrically conductive and is being affected by an electrostatic field applied via a suspending charged foil, the film becomes more unstable than that in a free-charged case because the pulling-over force induced by an electrostatic field acts as a destabilizing effect. The main application of this film flow comes from the new idea for the design of an electrostatic liquid film radiator (ELFR) rejecting heat in space [Kim et al., 1992, 1994]. In ELFR the elctrostatic field acts as an external attracting force to prevent leakage of the liquid-metal coolant through a puncture made by an unexpected accident such as a collision with a space debris or a micrometeorite. This new technique was proposed as a substitute for the present-day space radiator, which employs rather heavy armored heat pipes.

As a thin liquid layer drains under gravity down an inclined plane, it is susceptible to long surface-wave instabilities. The stability theories of thin film flows over an inclined plane under the action of gravity were first investigated by Benjamin [1957] and Yih [1963]. They identified regimes of linear stability as a function of the Reynolds number and the angle of inclination. The exponentially growing wave develops into the almost sinusoidal permanent traveling wave with small but equilibrium amplitude around the cutoff wavenumber. The study on the nonlinear stabilities was then extended by several authors [Benny, 1966; Gjevik, 1970; Lin, 1974; Tougou, 1981]. Lin [1974] performed a weakly nonlinear analysis near the critical Reynolds number and found a transition point separating supercritical from subcritical bifurcation. A supercritically stable wave is expected to be equilibrated into a single wave with a few lowest excited harmonics of its initial fundamental wave due to the nonlinear modal interaction. The result of their examinations is a nonlinear evolution equation for the layer thickness as a function of time. The analysis of a thin liquid layer has been extended to take into account the effect of an electrostatic field, and the basic question of how the thin liquid layer flowing down an inclined plane and an electrostatic field interact was answered by Kim et al. [1992].

The aim of the present work is to address the questions concerning the instabilities of the film flow affected by an electric field in the limit of long-wave approximation. For this purpose a strongly nonlinear evolution equation representing the film height is used for two-dimensional disturbances. From this equation the linear stability analysis is performed about the uniform film layer, and the nonlinear behavior of disturbances is investigated by a numerical computation using a Fourier-spectral method. And it will be shown that the initial disturbance modes in the nonlinear calculation are consistent with those obtained from the linear stability theory. The free-surface shapes and the Fourier-spectral coefficients are computed as time elapses. The electrostatic field (the strength is 1 KV/cm) is assumed to be uniformly distributed along the charged plate whose scale is also equal to the inclined plane (see Fig. 1).

The following sections are composed of formulation, linear stability analysis, nonlinear film evolution and conclusions. In the Sec. of formulation, the flow configuration and the governing system of equations in both of vacuum and liquid spaces are explained. Linear stability analysis for the transient, spatially uniform and basic state is performed, and the neutral and

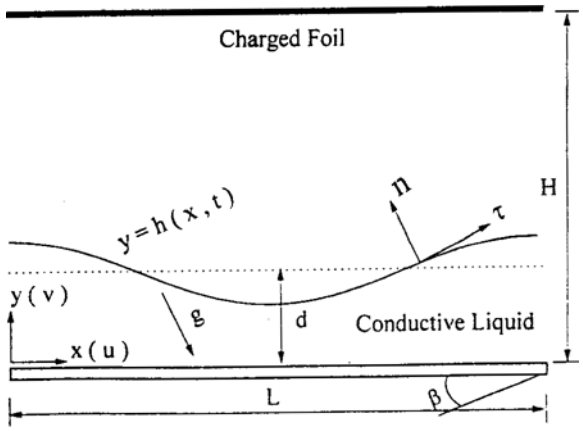

Fig. 1. The physical configuration of the plane flow under an electrostatic field.

the maximum growth rates are obtained in the Sec. of linear stability analysis. The various nonlinear instabilities for the two cases of Reynolds numbers are calculated in the Sec. of nonlinear film evolution and in the final Sec. the results are concluded.

FORMULATION

The layer is assumed incompressible, viscous and forms a thin liquid film flowing down an inclined plane under gravity g. Two-dimensional case is only considered and the plane is making an angle β with the horizontal. The coordinate system is chosen such that the x axis is parallel to the plane and the y axis is perpendicular to it. Above the liquid film there is a vacuum, where at a distance H from the plane is a charged plate of length L (see Fig. 1). Suppose that d is defined as the characteristic thickness of the primary film flow, then the following small parameter ξ denotes the film is very thin, that is,

$$\xi = d/L \ll 1. \tag{1}$$

If $d/H \ll 1$ then the charged plate is very far from the plane relative to the film thickness. Therefore, the electrostatic problem can be decoupled from the fluid dynamic problem.

1. Electric Potential

The electric potential is determined by solving the Laplace's equation,

$$\nabla^2 \phi = 0, \tag{2}$$

for the electric potential $\phi(x, y)$ in the fluid, ϕ^f, and for that in the vacuum region, ϕ^v. The fluid region is defined by $0 \le y \le h$ (x, t) and $-\infty < x < \infty$, where y=h(x, t) is the height of the film above the inclined plane, and the vacuum region is defined by the strip $-\infty < x < \infty$ and $h(x, t) \le y \le H$. To solve the Eq. (2) the following boundary conditions are needed:

$$\begin{aligned} &\phi(x, H) = FH\Phi(x), \text{ for } y = H, \\ &\phi = 0, \text{ for } y = 0. \end{aligned} \tag{3}$$

The function Φ(x) is a given dimensionless function of x, F denotes the unit of an electric strength and the product FH is a constant with the unit of electric potential. Along y=h(x, t) there are two more boundary conditions:

$$\phi^f(x, h, t) = \phi^v(x, h, t), \quad \varepsilon_f \frac{\partial \phi^f}{\partial n} = \varepsilon_v \frac{\partial \phi^v}{\partial n}. \tag{4}$$

Here ε_f is the dielectric constant of the fluid, ε_v is that of the vacuum, and the partial derivative is taken in the direction of the outward unit normal, **n**, to the interface. Unless no confusion can occur the subscript or superscript f is used for the quantities in the fluid region and v for the quantities in the vacuum region. Setting $H^*=H/d$ as a dimensionless foil height and $\zeta=H/L$, the dimensionless electric field vector can be written as

$$\vec{E} = \left(\zeta \frac{\partial \phi}{\partial x}, \; H^* \frac{\partial \phi}{\partial y} \right) \tag{5}$$

with the normal component defined as $E_n=\vec{E}\cdot\mathbf{n}$ and the tangential component as $E_t=\vec{E}\cdot\tau$, where τ is the unit tangent to the interface. The free-surface is unknown, so that the solution is coupled to the dynamics of the layer. In addition, to examine the interaction effect between the fluid media and an applied electrostatic field we have to consider the stress tensor σ_{ij} generated by the given electric field E [Landau et al., 1984],

$$\sigma_{ij} = -p_0(\rho, T)\delta_{ij} - \frac{E^2}{8\pi}\left[\varepsilon - \rho\left(\frac{\partial \varepsilon}{\partial \rho}\right)_T\right]\delta_{ij} + \frac{\varepsilon E_i E_j}{4\pi}, \tag{6}$$

where $p_0(\rho, T)$ is the pressure which would be found in the medium in the absence of a field and for given values of density ρ and the temperature T. The δ_{ij} stands for the Kronecker delta. If the medium is moving, then an additional deformation tensor due to the viscous effect will be included in (6). Thus an electric property, i.e., the permittivity ε of the medium affects the stability of the flow system. However, here the fluid will be treated as an incompressible conductor at an isothermal condition. Therefore the electric properity will not affect the thin film flow. Generally as the property ε has small values such as in dielectrics, the effect of the stress becomes weak.

2. Equations of Fluid Motion

The liquid layer is governed by the Navier-Stokes equations. Letting d be the unit of length in the y direction, L the unit of length in the x direction, U_0 the unit of velocity in the x, direction, ξU_0 the unit of velocity in the y direction, L/U_0 the unit of time, ρU_0^2 the unit of pressure, ρ the fluid density, ε_v the unit of the dielectric constant, and μ the fluid viscosity, the dimensionless governing equations of motion become

$$u_x + v_y = 0, \tag{7}$$

$$\xi(u_t + uu_x + vu_y) = -\xi p_x + \frac{1}{Re}(\xi^2 u_{xx} + u_{yy}) + \frac{\sin\beta}{Fr^2}, \tag{8}$$

$$\xi^2(v_t + uv_x + \xi v v_y) = -p_y + \frac{\xi}{Re}(\xi^2 v_{xx} + v_{yy}) - \frac{\cos\beta}{Fr^2}. \tag{9}$$

Here u and v are the velocity components of x and y directions, respectively, and p is the pressure. The subscripts represent the partial derivatives. The dimensionless groups Re and Fr are introduced for the Reynolds number and the Froude number, and defined as

$$Re = \frac{\rho U_0 d}{\mu}, \tag{10}$$

$$Fr=\frac{U_0}{\sqrt{gd}}. \tag{11}$$

There are two kinds of boundary conditions, i.e., one is on the solid wall and the others are on the free surface. The no-slip boundary condition at y=0 is given by

$$u=v=0. \tag{12}$$

On the free surface y=h(x, t), the kinematic condition is

$$h_t+u\,h_x=v \tag{13}$$

and the continuity of the tangential and normal stresses [Landau et al., 1984] are, respectively,

$$(1-\xi^2h_x^2)\,(u_y+\xi^2v_y)+2\xi^2h_x(v_y-u_x)=0, \tag{14}$$

$$\frac{\xi^2}{Ca}\frac{h_{xx}}{(1+\xi^2h_x^2)^{3/2}}=-\frac{Re}{2}p+K\left(\frac{1}{\varepsilon_f}-1\right)(E_n^{v2}+\varepsilon_f E_t^{v2})$$
$$+\xi\{\xi^2h_x^2u_x-h_x(u_y+\xi^2v_x)+v_y\}\,(1+\xi^2h_x^2)^{-1}, \tag{15}$$

where the capillary number Ca to take into account the surface tension σ and the dimensionless constant K are defined as

$$Ca=2\mu U_0/\sigma,$$
$$K=\varepsilon_v dF^2/16\pi\mu U_0. \tag{16}$$

The pressure in the vacuum is set to zero.

LINEAR STABILITY ANALYSIS

First, assuming the Reynolds number is order unity, the evolution equation for h(x, t) accurate to $O(\xi^2)$ can be determined in the thin film limit. The characteristic unit of velocity is defined as equal to the mean velocity of the basic plane flow down in the inclined plane, i.e., $U_0=\rho g d^2\sin\beta/3\mu$. Keeping terms upto the order ξ in (7)-(15) and using asymptotic expansions of the dependent variables for small ξ, the velocity components u and v on the free surface are determined

$$u(t, x, h)=\frac{3}{2}h^2+\xi\left(\frac{5}{18}Re\,h^3h_x-\frac{3}{2}h_x\cot\beta+\frac{\xi^2}{Ca}h_{xxx}+K\frac{\partial E_{0n}^{v2}}{\partial x}\right)$$
$$h^2+O(\xi^2), \tag{17}$$

$$v(t, x, h)=-\frac{3}{2}h^2h_x-\xi\left[Re\,h^3\left(\frac{6}{5}h_{xx}+\frac{213}{40}h_x^2\right)\right.$$
$$-\cot\beta\left(h_{xx}+\frac{3}{2}h_x^2\right)+\frac{\xi^2}{Ca}\left(\frac{2}{3}hh_{xxxx}+h_xh_{xxx}\right)$$
$$\left.+K\left(\frac{2}{3}\frac{\partial^2E_{0n}^{v2}}{\partial x^2}h+\frac{\partial E_{0n}^{v2}}{\partial x}h_x\right)\right]h^2+O(\xi^2), \tag{18}$$

where $\xi^2/Ca=O(1)$ and

$$E_{0n}^{v}=H^*\Phi(x)\frac{\partial}{\partial y}\{1+(y-H^*)[h(1/\varepsilon_f-1)+H^*]^{-1}\}$$
$$\text{on } y=h(x, t), \tag{19}$$

and finally substituting (17) and (18) into the kinematic condition (13) the evolution equation for the first two orders in ξ is obtained such as

$$h_t+3h^2h_x+\xi\frac{\partial}{\partial x}\left(\frac{6}{5}Re\,h^6h_x-h^3h_x\cot\beta+\frac{2}{3}\frac{\xi^2}{Ca}h^3h_{xxx}\right)$$
$$+\frac{4}{3}\xi h^2K\left(1-\frac{1}{\varepsilon_f}\right)\cdot$$
$$\left[3h_xE_{0n}^{v}\frac{\partial E_{0n}^{v}}{\partial x}+h\left(\frac{\partial E_{0n}^{v2}}{\partial x}+E_{0n}^{v}\frac{\partial^2E_{0n}^{v}}{\partial x^2}\right)\right]=0. \tag{20}$$

Next, to perform a linear stability analysis the Eq. (20) is perturbed about its steady-state solution, i.e., $h(x, t)=1+h_1(x, t)$ with assuming $\Phi(x)=1$. The small disturbance h_1 is assumed to have a simple harmonic form, i.e., $h_1=\exp\{i\alpha(x-ct)\}$, where $\alpha\geq0$ is the wavenumber of the disturbance and c is the complex wave speed, i.e., $c=c_r+ic_i$.

After h_1 is put into (20), it yields the critical Reynolds number

$$Re_c=\frac{5}{6}\cot\beta+\frac{5}{9}\frac{\xi^2}{Ca}\alpha^2-\frac{10}{9}K\left(\frac{1}{\varepsilon_f}-1\right)W, \tag{21}$$

where

$$W=\frac{\alpha H^{*2}(1/\varepsilon_f-1)}{(H^*+1/\varepsilon_f-1)^2}\left\{\tanh[\alpha(H^*-1)]+\frac{\tanh\alpha}{\varepsilon_f}\right\}^{-1}. \tag{22}$$

When surface tension and electrostatic field are neglected, Eq. (21) has the same condition for the neutral stability obtained by Benjamin [1957] and Yih [1963].

In addition, the maximum growth rate showing the maximum rate of amplification of surface-wave disturbance is also attained in (α, Re) domain after plugging $h_1=\exp\{i\alpha(x-ct)\}$ into Eq. (20) and computing $d(\alpha C_i)/d\alpha=0$, i.e.,

$$Re=\frac{5}{6}\cot\beta+\frac{10}{9}\frac{\xi^2}{Ca}\alpha^2-\frac{5}{9}K\left(\frac{1}{\varepsilon_f}-1\right)\left(2W+\alpha\frac{dW}{d\alpha}\right). \tag{23}$$

The cutoff wavenumber α_c from (21) and maximum-growth-rate wavenumber α_m from (23) are plotted corresponding to Re in Fig. 2 for both F=1 KV/cm (dashed line) and F=0 KV/cm (solid line), $H^*=13.3$, $\beta=30^\circ$, g=1 cm/sec^2 and with the physical parameters for lithium at 700 K ($\mu=0.0038$ p, $\sigma=363.2$ dyn/cm and $\rho=0.493$ g/cm^3). Later the wavenumbers within the unstable region at Re=9.5 (d=0.15 cm) will be used for the nonlinear computations of the surface-wave evolution to confirm whether the expectation from this linear stability analysis is true or not. The effect of an electrostatic field increases both wavenumbers showing a maximum linear growth rate and a cutoff at a given Reynolds number. When the effect of electrostatic field is ignored, (21) and (23) yield the same results obtained by Gjevik [1970].

NONLINEAR FILM EVOLUTION

The linear analysis in the previous section is only valid as

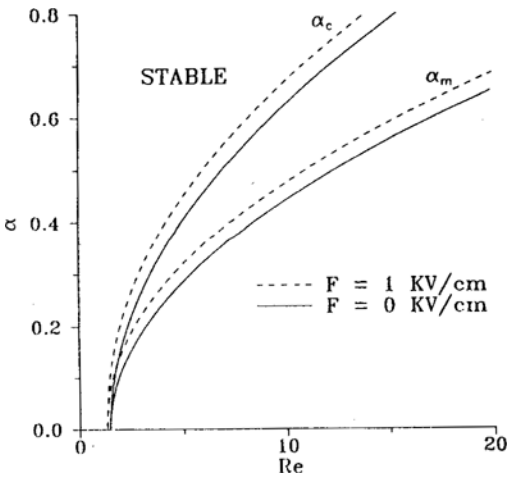

Fig. 2. Linear stability curves in the (α, Re)-plane for β=30°, H= 2 cm, K=1.44 and Ca=1.02×10^{-5}.

long as the disturbed amplitudes are maintained as small as possible. Thus to see the nonlinear evolution of surface wave , Eq. (20) has to be solved numerically. In an analytical point of view the nonlinear equation has been examined by Gjevik [1970], Lin [1974] and Tougou [1981] to name only a few. Gjevik [1970] and Tougou [1981] took into account waves having the initial wavenumbers close to the cutoff $\alpha=\alpha_c$ and analyzed by taking the fundamental mode and its lowest harmonics. Lin [1974] performed a weakly nonlinear analysis near the critical Reynolds number and found a transition point α_s (around $\alpha_c/2$) separating (α, Re)-plane into supercritical ($\alpha>\alpha_s$) and subcritical ($\alpha<\alpha_s$). When $\alpha>\alpha_s$ the capillary force is dominating and the flow becomes stable, i.e., supercritically stable. If α is near α_s, the equilibrated wave has a form similar to a single wave observed by Kapitza and Kapitza [1949] and studied analytically by Pumir et al. [1983]. When $\alpha<\alpha_s$ the flow is not equilibrium because the harmonics with higher frequency are largely excited under nonlinear modal interactions.

In the laterally unbounded domain the evolution Eq. (20) becomes an initial value problem, where the initial wave is imparted as a sinusoidal disturbance imposed on the flat interface:

$$h(x, 0)=1-\bar{h}\cos(\alpha x), \tag{24}$$

where $\bar{h}$ is set 0.1. This makes the computational domain periodic and the Fourier-spectral method [Gottlieb and Orszag, 1977] is helpful to solve the evolution equation numerically. The film height h(x, t) is calculated by a finite Fourier series

$$h(x, t)=\sum_{n=-N}^{n=N} a_n(t)\exp\{i\alpha n x\}+c.c \tag{25}$$

with $N\geq 64$. The c.c means the complex conjugate. The computational domain is set to the range, $-\pi/\alpha\leq x\leq\pi/\alpha$. The time marching of the solution is performed by virtue of a fourth-order modified Hamming's predictor-corrector method with the maximum tolerance of 10^{-11} using the fourth-order Runge-Kutta method. At each time step the spectral coefficient $a_n(t)$ is computed for monitoring the surface deformation. To eliminate the aliasing data errors, that is, poor representations of the true function because the space step Δx is too large, a large number

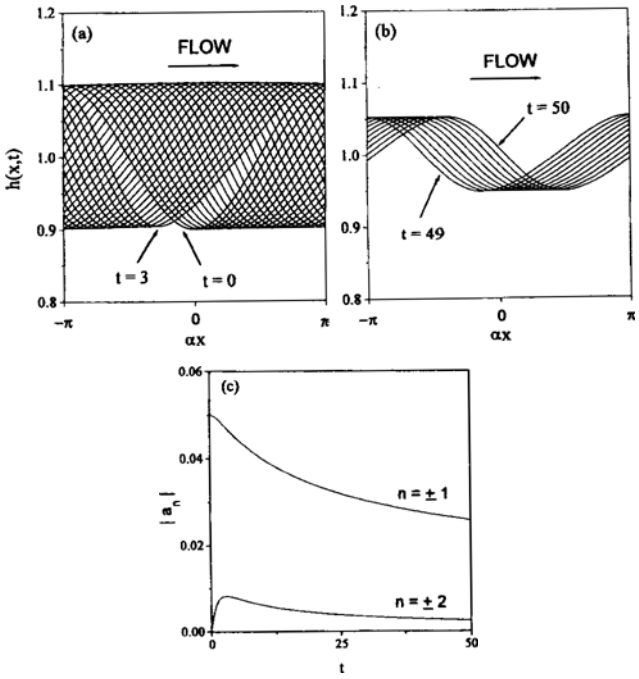

Fig. 3. Surface-wave instability for α=0.64, Re=9.5, K=1.44 and Ca=1.02×10^{-5}.
(a) free-surface configurations for $0\leq t\leq 3$ with Δt=0.1,
(b) free-surface configurations for $49\leq t\leq 50$ with Δt=0.1,
(c) evolution of Fourier-spectral coefficients.

of collocation points are taken and the upper half of the Fourier modes are discarded. The evolution of interface has been computed with several starting wavenumbers, i.e., from around the neutral stability to instability, obtained by the linear stability analysis by setting ξ=0.02 to meet the assumed long-wave approximation. The Eq. (20) is now solved for Re=9.5, K=1.44(F=1 KV/cm) and Ca=1.02×10^{-5}. In this case α_c=0.65 and α_m=0.46. Fig. 3 shows the surface-wave instability with the imparting disturbance wavenumber α=0.64 in the vicinity of the cutoff. It is suggested that the surface deformation be linearly unstable because this wavenumber (slightly smaller than the cutoff) is located in the unstable region as seen in Fig. 2. In Fig. 3(a) the disturbance grows linearly for small time but soon it reaches a maximum value and then decays with the growth of the lowest harmonics (n=±2). The harmonics distort the initial sinusoidal shape as time elapses and the magnitude of the surface wave decreases monotonically after the maximum with the wave front steepening and the wave rear stretching as shown in Fig. 3(b). The free surfaces are plotted at every t=0.1. In Fig. 3(c), the magnitudes of the fundamental and lower harmonics (n=±2) are plotted. The modes higher than n=±2 are so small that they are not computed.

In Fig. 4 the free-surface deformations are plotted with $\alpha=\alpha_m$. Fig. 4(a), 4(b) and 4(c) show the free-surface evolutions for initial growth, intermediate decay and equilibration, respectively. Each line is calculated at every time increment of 0.1. As we can infer from the linear stability theory the initial wave growth is much more obvious than that in the previous case. In the intermediate evolution the decay rates of the excited harmonics distort the free-surface waves prominently as shown in Fig.

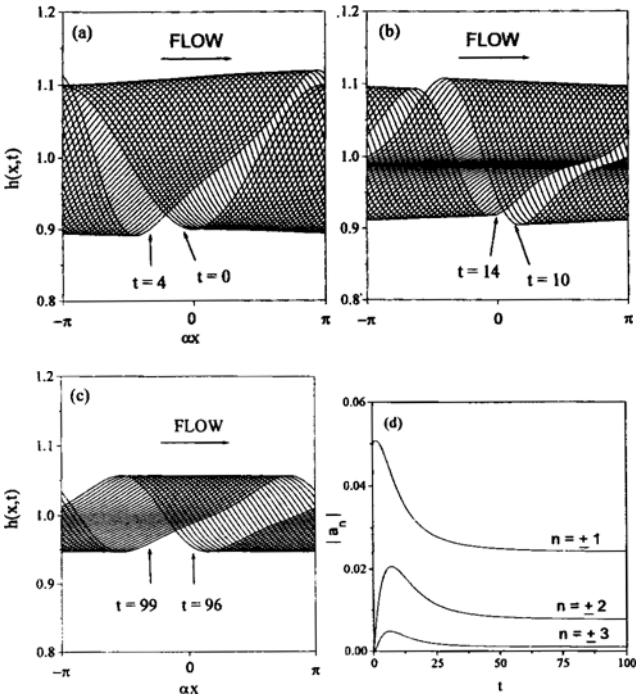

Fig. 4. Surface-wave instability for $\alpha=\alpha_m=0.46$, Re=9.5, K=1.44 and $Ca=1.02\times10^{-5}$.
(a) free-surface configurations for $0\leq t\leq 4$ with $\Delta t=0.1$,
(b) free-surface configurations for $10\leq t\leq 14$ with $\Delta t=0.1$,
(c) free-surface configurations for $96\leq t\leq 99$ with $\Delta t=0.1$,
(d) evolution of Fourier-spectral coefficients.

4(b). In the equilibration stage shown in Fig. 4(c) the wave has a permanent form with the dimples generated due to harmonics. The spectral coefficients are plotted in Fig. 4(d) and the limiting values are equilibrated with larger magnitudes compared to the previous ones. Therefore from these modes it can be deduced the eventual wave is slightly distorted but permanently periodic. The modes higher than ±3 are very small.

Fig. 5 shows how the supercritically stable surface waves are transformed from an initial wave-flow state with a decreased wavenumber. The initial disturbance wavenumber is smaller than α_m but a little larger than α_s(=0.325), i.e., α=0.365, where more significant contributions of the harmonics are expected. The initial growth and the subsequent decay of the free surface are similar to the previous case except that the fundamental modes and the second higher modes are met each other around t=25 and the modes are not monotonically converging to limit values. The intermediate free-surface configurations are plotted in Fig. 5(a). As time marches the modes are interacting with each other and rearrange their magnitudes to have a permanent wave as shown in Fig. 5(b) and this resembles the single wave computed by Pumir et al. [1983], that is, the permanent wave with reduced smaller wavelength is evolved through nonlinear modal self-interaction of a monochromatic wave disturbance imparted initially under the electrostatic field. The modes are calculated upto n=±4 as shown in Fig. 5(c).

Fig. 6 shows the surface-wave instability for α=0.33, which is very close to α_s. According to the weakly nonlinear analysis this flow system becomes equilibrium as in the previous case although the evolution modes area little different. Fig. 6(a-c)

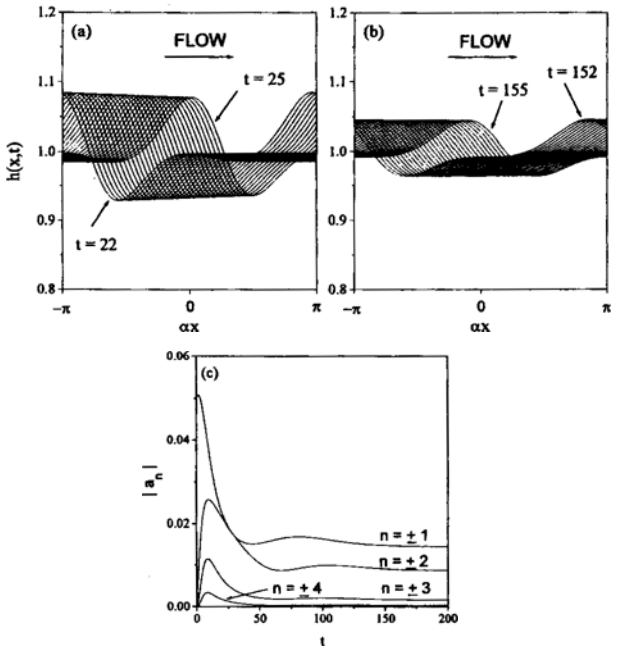

Fig. 5. Surface-wave instability for α=0.365, Re=9.5, K=1.44 and $Ca=1.02\times10^{-5}$.
(a) free-surface configurations for $22\leq t\leq 25$ with $\Delta t=0.1$,
(b) free-surface configurations for $152\leq t\leq 155$ with $\Delta t=0.1$,
(c) evolution of Fourier-spectral coefficients.

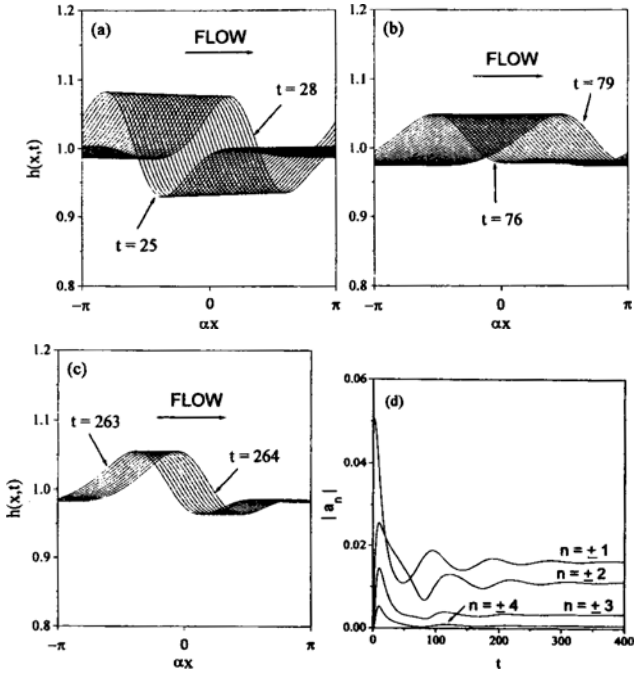

Fig. 6. Surface-wave instability for α=0.33, Re=9.5, K=1.44 and $Ca=1.02\times10^{-5}$.
(a) free-surface configurations for $25\leq t\leq 28$ with $\Delta t=0.1$,
(b) free-surface configurations for $76\leq t\leq 79$ with $\Delta t=0.1$,
(c) free-surface configurations for $263\leq t\leq 264$ with $\Delta t=0.1$,
(d) evolution of Fourier-spectral coefficients.

shows the free-surface shapes for time step of 0.1, while Fig. 6(d) represents the evolution of the first four spectral coef-

ficients. Fig. 6(a) shows the crests of the surface waves decay due to the lost of energy while the dimples are significantly growing. This fact can be explained from the evolution of Fourier-spectral modes, i.e., as seen in Fig. 6(d) the fundamental modes are decreasing more rapidly than the modes n=±2 in the computational time range used in Fig. 6(a), t=25-t=28. In Fig. 6(b) the fundamental modes recapture the energy and dominate again, while the lower harmonics are still decaying. Hence we can see the crests are growing while the dimples are disappearing. After the initial crests grow and decay several more times with the harmonics undulating, the free surface becomes permanent as shown in Fig. 6(c).

In Fig. 7, the surface-wave instability has been calculated at $\Delta t=0.1$ with the initial disturbance wavenumber $\alpha=0.2$. In the initial stage of instability the amplitude of the disturbance increases exponentially according to the linear stability theory, but soon grows super-exponentially as in Fig. 7(a). The rapid evolution and growth of the harmonics excited from earlier stage-

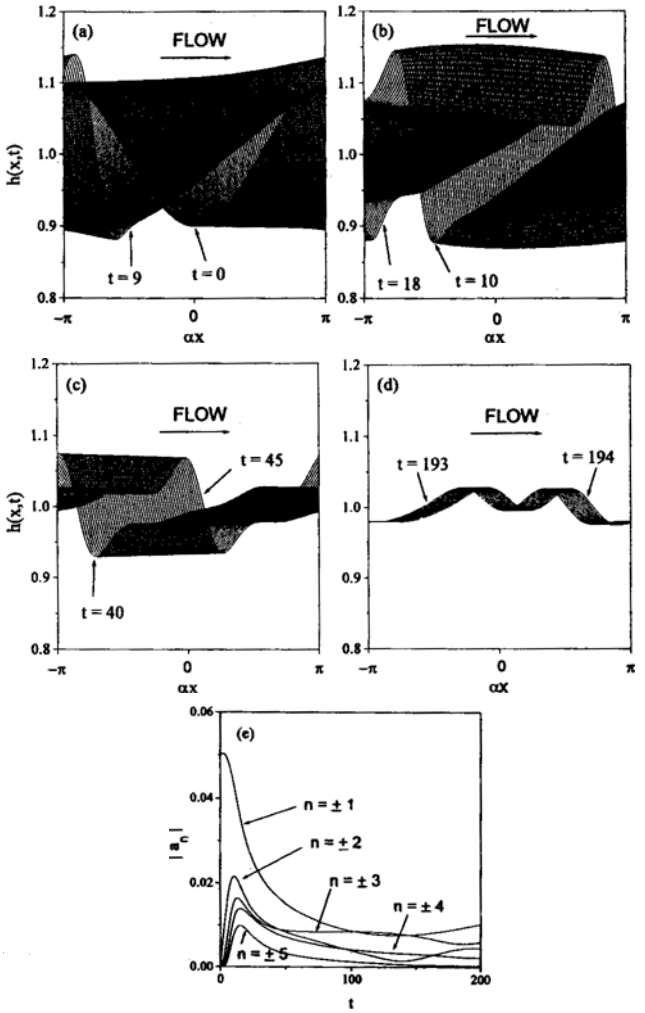

Fig. 7. Surface-wave instability for $\alpha=0.2$, Re=9.5, K=1.44 and $Ca=1.02\times10^{-5}$.
(a) free-surface configurations for $0\le t\le 9$ with $\Delta t=0.1$,
(b) free-surface configurations for $10\le t\le 18$ with $\Delta t=0.1$,
(c) free-surface configurations for $40\le t\le 45$ with $\Delta t=0.1$,
(d) free-surface configurations for $193\le t\le 194$ with $\Delta t=0.1$,
(e) evolution of Fourier-spectral coefficients.

make the wave fronts steeper and the rears stretching. This phenomena makes dimples later as in Fig. 7(b), where as dimples appear on the longer rears the amplitude of free surface gets smaller after reaching a maximum. As time elapses this surface-wave deformation gets more significant. Therefore, as this process develops the flow system has growing dimples while the initial crests are decaying continuously, as shown in Fig. 7(c). Fig. 7(d) shows for sufficiently large time the initial crests and the generated dimples have almost equal values in the magnitudes of fee-surface waves. The competition between the fundamental and the harmonics continues through the nonlinear modal self-interaction. Fig. 7(e) represents the evolution of Fourier-spectral coefficients upto n=±5. The higher modes excited initially become important and controlthe flow system far away from the bifurcation point.

At sufficiently large Re catastrophic surface waves have been observed by Pumir et al. [1983]. Thus to confirm this behavior in the film flow under an electrostatic field, the characteristic film height d has been further increased to 0.2 cm while the other parameters are kept as the same values in the previous computations. In this case the newly calculated values of the dimensionless groups are Re=22.44, K=1.08 and $Ca=1.81\times10^{-5}$ which yield the cutoff wavenumber $\alpha_c=1.4$ and the wavenumber at the maximum growth rate $\alpha_m=1.0$. As an example case the nonlinear computations are performed at $\alpha=0.68$, where the flow system will be unstable. Fig. 8 shows the surface-wave instability of this film flow. Fig. 8(a), 8(b) and 8(c) represent the evolution of free-surface shapes for initial, intermediate growth and wavebreaking, respectively. Each line stands for

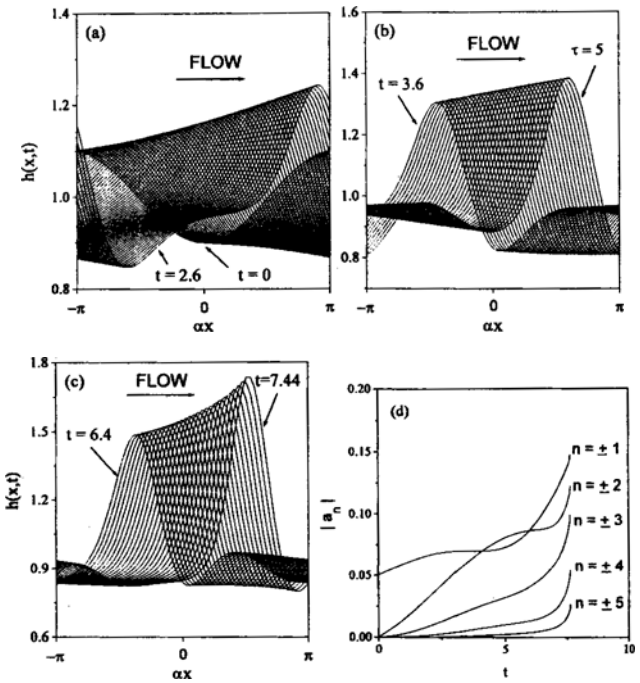

Fig. 8. Surface-wave instability for $\alpha=0.68$, Re=22.44, K=1.08 and $Ca=1.81\times10^{-5}$.
(a) free-surface configurations for $0\le t\le 2.6$ with $\Delta t=0.04$,
(b) free-surface configurations for $3.6\le t\le 5$ with $\Delta t=0.04$,
(c) free-surface configurations for $6.4\le t\le 7.44$ with $\Delta t=0.04$,
(d) evolution of Fourier-spectral coefficients.

the time increment of 0.04. Fig. 8(d) shows the evolution of the first five Fourier-spectral coefficients. In Fig. 8(a), the amplitude of the disturbance grows super-exponentially due to the higher harmonics excited in the initial stage. The rapid evolution of the free-surface configuration makes the wave fronts steeper and generate dimples on the rear-wave sites. In Fig. 8(b), the growth of the dimples is significant because the modes $n=\pm 2$ gains energy from the fundamental. As the film height gets thicker, the local phase speed of the wave is accelerating. Therefore, the traveling speed of the crests is greater than that of the troughs, as shown in Fig. 8(c) where the fundamental recaptures the energy and dominates, resulting in making the wave fronts steeper and steeper. Accordingly the surface-wave soon breaks and shows a catastrophic behavior. And the computation work is terminated at t=7.44.

The nonlinear film evolution has been calculated with various wavenumbers and the free-surface growth rates are monitored by the Fourier-spectral coefficients. For small evolution time the growth rates are consistent with the results obtained from the linear disturbance theory. The differences in the nonlinear growth rates have been shown in Figs. 3-8, and the growing rates of the wave crests are much larger than the thinning rates of the troughs which can be anticipated by examining the vertical component of the velocity (18) at the interface, that is, the driving force mainly depends on powers of the film height h and thus has much more influence on the thicker region. The effect of an electrostatic force destabilizes the flow system and hence it gives larger wavenumbers for both cutoff and maximum growth rate in the linear stability region as shown in Fig. 2. The film flow without the effect of an electrostatic field has been studied by Burelbach et al. [1988] and Joo et al. [1991] for the isothermal and the nonisothermal cases. In the nonisothermal case the film flow on the heated inclined plane is considered in surface-wave and thermocapillary instability.

CONCLUSIONS

The evolution equation representing the electrohydrodynamics has been used for the linear stability analysis about the uniform film layer. Because the applied electrostatic tensile stress tends to destabilize the liquid film flow, the instability region in (α, Re)-plane is broader compared to the free-charged film flow. The nonlinear behavior is investigated in a periodic domain by computing the free-surface configuration and the Fourier-spectral coefficients numerically. For small time the surface-wave instability modes are consistent with the results obtained from the linear stability theory for $\alpha<\alpha_c$ and $Re>Re_c$. When the initial disturbance wavenumber is within the supercritically stable region, i.e., $\alpha_s<\alpha<\alpha_c$ and $Re>Re_c$, we can see the flow system finally equilibrates and develops a permanent wave according to the convergence of the harmonics. In proportion to the decrease of the wavenumber into the subcritical region the rearranged surface-wave has no equilibration since the higher harmonics are important through the nonlinear modal self-interaction. If Reynolds number increases owing to the film thickness, the local phase speed gets higher and hence the wave crests travel much faster than the troughs on the wave rears as shown in Fig. 8. Accordingly, the wavebreaking phenomena has been observed at sufficiently large Reynolds number.

This study has been performed only based on the two-dimensional disturbance theory. To have access to more physical justification the stability behavior needs to be considered for three-dimensional disturbance with streamwise and spanwise wavenumbers. This kind of question will be addressed in later study.

ACKNOWLEDGMENT

This work was partially supported by Seoul City University and the author thanks it.

NOMENCLATURE

Ca : capillary number
c : complex wave speed
d : characteristic film thickness [cm]
$\vec{E}$: electric field vector
F : characteristic unit of electric field [KV/cm]
Fr : Froude number
g : gravity [cm/sec^2]
H : distance from plane to charged foil [cm]
H* : dimensionless foil height
h : free-surface thickness [cm]
h_1 : perturbed dimensionless film thickness
$\bar{h}$: dimensionless initial film disturbance
K : $\varepsilon_v dF^2/16\pi\mu U_0$
L : characteristic length scale parallel to plane [cm]
N : number of modes in Fourier series
n : unit normal vector to the interface h
p : pressure [dyne/cm^2]
Re : Reynolds number
T : temperature [K]
t : time [sec]
U_0 : characteristic unit of velocity in x direction
u : velocity component of x direction [cm/sec]
v : velocity component of y direction [cm/sec]
x : distance coordinate parallel to plane [cm]
y : distance coordinate perpendicular to plane [cm]

Greek Letters

α : wavenumber
β : inclination angle of plane with the horizontal
δ_{ij} : Kronecker delta
ε : dielectric constant
ζ : H/L
μ : fluid viscosity
ξ : d/L
ρ : fluid density
σ : surface tension
σ_{ij} : stress tensor
τ : unit tangent vector to the interface h
Φ : dimensionless electric potential along y=H
ϕ : electric potential [KV]

Superscripts

f : fluid
v : vacuum

Subscripts

c : critical value
f : fluid
i : imaginary part
m : maximum growth rate
r : real part
s : supercritical value
t : partial derivative with t
v : vacuum
x : partial derivative with x
y : partial derivative with y

REFERENCES

Benjamin, T. B., "Wave Formation in Laminar Flow Down an Inclined Plane", *J. Fluid Mech.*, **2**, 554 (1957).

Benney, D. J., "Long Waves on Liquid Films", *J. Math. Phys.*, **45**, 150 (1966).

Burelbach, J. P., Bankoff, S. G. and Davis, S. H., "Nonlinear Stability of Evaporating/Condensing Liquid Films", *J. Fluid Mech.*, **195**, 463 (1988).

Gjevik, B., "Occurrence of Finite-Amplitude Surface Waves on Falling Liquid Films", *Phys. Fluids*, **13**, 1918 (1970).

Gottlieb, D. and Orszag, S. A., "Numerical Analysis of Spectral Methods: Theory and Applications", SIAM, Philadelphia, Pennsylvania, 1977.

Joo, S. W., Davis, S. H. and Bankoff, S. G., "Long-wave Instabilities of Heated Falling Films: Two-dimensional Theory of Uniform Layers", *J. Fluid Mech.*, **230**, 117 (1991).

Kapitza, P. L. and Kapitza, S. P., "Wave Flow of Thin Layers of a Viscous Fluid", *Zh. Ek. Teor. Fiz.*, **19**, 105 (1949).

Kim, H., Bankoff, S. G. and Miksis, M. J., "The Cylindrical Electrostatic Liquid Film Radiator for Heat Rejection in Space", *J. of Heat Transfer*, **116**, 986 (1994).

Kim, H., Bankoff, S. G. and Miksis, M. J., "The Effect of an Electrostatic Field on Film Flow Down an Inclined Plane", *Phys. Fluids A*, **4**, 2117 (1992).

Kim, H., Miksis, M. J. and Bankoff, S. G., "The Electrostatic Liquid-Film Radiator for Heat Rejection in Space", *Topics in Heat Transfer*, HDT-**206-3**, ASME, 35 (1992).

Landau, L. D., Lifshitz, E. M. and Pitaevskii, L. P., "Electrodynamics of Continuous Media", 2nd ed., Pergamon, New York, 1984.

Lin, S.-P., "Finite Amplitude Side-Band Stability of a Viscous Film", *J. Fluid Mech.*, **63**, 417 (1974).

Pumir, A., Manneville, P. and Pomeau, Y., "On Solitary Waves Running Down an Inclined Plane", *J. Fluid Mech.*, **135**, 27 (1983).

Yih, C.-S., "Stability of Liquid Flow Down an Inclined Plane", *Phys. Fluids*, **5**, 321 (1963).